International Journal of
MATERIALS RESEARCH

Zeitschrift für METALLKUNDE

Feature

Thomas Hammerschmidt[a], Ralf Drautz[a], David G. Pettifor[b]
[a] ICAMS, Ruhr-Universität Bochum, Bochum, Germany
[b] Department of Materials, University of Oxford, Oxford, United Kingdom

Atomistic modelling of materials with bond-order potentials

The atomistic modelling of materials with effective model potentials requires a reliable description of the breaking and making of interatomic bonds in different atomic environments. The bond-order potentials provide such a transferable description of atomic bonding while at the same time they are computationally efficient for application in large-scale atomistic simulations. We give an overview of the fundamentals of bond-order potentials and their derivation from the tight-binding electronic structure by linking the atomic structure to the electronic structure. We discuss the application of the structural energy difference theorem for studying trends in crystal phase stability and provide a brief summary of representative examples for modelling metals, hydrocarbons, and semiconductors with analytic and numerical bond-order potentials.

Keywords: Atomistic modelling; Bond-order potentials; Crystal phase stability

1. Introduction

The design and fabrication of modern technological materials is challenging due to the combinatorial diversity of multi-component systems. A reliable description of the thermodynamic stability and metastability of compound phases and the kinetics of phase formation can contribute to make this task more tractable. For the prediction of materials behaviour during service one needs an accurate understanding of micro-mechanical properties, defect formation and structural transformations.

Reliable modelling on the atomistic scale requires effective interatomic potentials that capture the relevant properties of the system at hand. The particular requirements depend on the system but can be categorised in the following challenges for developing interatomic potentials: the potentials should be transferable to different bonding situations and computationally efficient for large-scale simulations. Moreover, the description of the interatomic interactions should be physically transparent to allow for a meaningful analysis of simulation data and to relate the chemistry of bond formation to phase stability. A realistic description of charge transfer and magnetism should be incorporated into the potential.

The bond-order potentials (BOPs) are a class of interatomic potentials that fulfil these demands. They are derived from quantum mechanics and provide a similar accuracy and transferability as tight-binding calculations at a smaller computational effort. The central entities of the BOPs are the bond order or density matrix and the local electronic density of states. By varying the bandfilling, one may analyse crystal structure stability as a function of the number of valence electrons. The explicit incorporation of the valence dependence of bond formation in the bond-order potentials means that charge transfer and magnetism may be taken into account in a physically transparent way.

The bond-order potentials are derived by coarse graining the electronic structure in two steps.

1. In the first step, the energy within density functional theory (DFT) is approximated by the tight-binding (TB) bond model [1]. The TB approximation is transferable to different crystal structures and allows for a physically transparent interpretation of atomic bonding.

2. In the second step, the electronic structure of the TB approximation is coarse grained into atom-based moments and bond-based interference paths for the derivation of effective interatomic interactions, the bond-order potentials.

In the following we will discuss the derivation of the potentials from the tight-binding description of the electronic structure to effective interatomic interactions.

In the first part of this paper, we introduce the tight-binding bond model followed by a brief outline of the central ideas and concepts of numerical and analytic bond-order potentials. The last part is devoted to applications of bond-order potentials for modelling metals, hydrocarbons, and semiconductors.

Comprehensive discussions of fundamentals and applications of bond-order potentials are given in recent reviews [2–5], a tutorial-like approach to bond-order potential theory was compiled by two of us recently [6].

2. Background

The theory of bond-order potentials starts from the tight-binding approximation that expresses the eigenfunctions ψ_n of the Schrödinger equation

$$\hat{H}\psi_n = E_n\psi_n \tag{1}$$

in a minimal basis centred on atoms i

$$|\psi_n\rangle = \sum_{i\alpha} c_{i\alpha}^{(n)} |i\alpha\rangle \tag{2}$$

where α denotes the orbital. For an orthonormal basis, the eigenvalues E_n and the coefficients $c_{i\alpha}^{(n)}$ of the eigenfunctions ψ_n are determined by solving the secular equation

$$\sum_{j\beta} H_{i\alpha j\beta} c_{j\beta}^{(n)} = E_n c_{i\alpha}^{(n)} \tag{3}$$

The diagonalisation of the Hamiltonian matrix

$$H_{i\alpha j\beta} = \langle i\alpha|H|j\beta\rangle \tag{4}$$

is the computationally most demanding part of tight-binding calculations. The matrix elements $H_{i\alpha j\beta}$ are expressed as functions of the interatomic distance and the atomic environment [7]. In the tight binding bond model [1], the binding energy of the system is given as the sum over covalent bond energy U_{bond}, repulsive energy U_{rep} and promotion energy U_{prom}

$$U_B = U_{\text{bond}} + U_{\text{prom}} + U_{\text{rep}} \tag{5}$$

where contributions from magnetism and charge transfer were not taken into account. The repulsive energy U_{rep} is often approximated as a pairwise contribution. The promotion energy U_{prom} is given by

$$U_{\text{prom}} = \sum_{i\alpha} E_{i\alpha}^{(0)} \left(N_{i\alpha} - N_{i\alpha}^{(0)}\right) \tag{6}$$

where $N_{i\alpha}$ denotes the number of electrons in orbital $|i\alpha\rangle$ and the superscript (0) refers to the atomic reference state. The bond energy U_{bond} can be expressed in terms of atom-based information or bond-based information. The so-called onsite and intersite representations are equivalent but offer different views on the bond formation in materials. Both representations are based on the coefficients of the eigenfunctions $|\psi_n\rangle$ of the Hamilton operator $\hat{H}$. The onsite representation is based on the atom-based local density of states (DOS) $n_{i\alpha}$ on atom $i\alpha$

$$n_{i\alpha}(E) = \sum_n \left|c_{i\alpha}^{(n)}\right|^2 \delta(E - E_n) \tag{7}$$

The intersite representation is expressed in terms of the bond-order $\Theta_{i\alpha j\beta}$ or the density matrix $\rho_{i\alpha j\beta}$ between orbital α on atom i and orbital β on atom j and is given by the sum over the occupied states

$$\Theta_{i\alpha j\beta} = 2\rho_{i\alpha j\beta} = 2\sum_n^{\text{occ}} c_{i\alpha}^{*(n)} c_{j\beta}^{(n)} \tag{8}$$

The bond energy in the onsite and intersite representation is given by

$$U_{\text{bond}} = 2\sum_{i\alpha} \int^{E_F} (E - E_{i\alpha})\, n_{i\alpha}(E)\, \mathrm{d}E \tag{9}$$

$$= \sum_{i\alpha \neq j\beta} \Theta_{i\alpha j\beta} H_{i\alpha j\beta} \tag{10}$$

where E_F is the Fermi level. An in-depth discussion and interpretation of the bond order for molecules and solids is given in the textbook of Pettifor [8].

3. Bond-order potentials

The central aim of BOP theory is to provide a local, physically transparent description of bond formation. Therefore, the diagonalisation of the Hamilton matrix in the tight-binding problem (Eq. (3)) needs to be replaced by a local evaluation of the density of states on an atom or the bond order between a pair of atoms. The key steps to achieve a local view on bond formation will be outlined in the following.

3.1. Relation of the crystal structure to the electronic structure

The moments theorem [9] is used to relate the local density of states $n_{i\alpha}(E)$ on orbital α of atom i to products of the matrix elements of the Hamilton operator $H_{i\alpha j\beta}$:

$$\begin{aligned}\mu_{i\alpha}^{(N)} &= \int E^N n_{i\alpha}(E)\, \mathrm{d}E \\ &= \langle i\alpha|\hat{H}^N|i\alpha\rangle \\ &= \sum_{j\beta k\gamma\cdots} H_{i\alpha j\beta} H_{j\beta k\gamma} H_{k\gamma\ldots} \cdots H_{\ldots i\alpha}\end{aligned} \tag{11}$$

Thus, the N-th moment of atom i, $\mu_i^{(N)}$, establishes a direct connection between the electronic structure of orbital α of atom i and the crystal structure surrounding atom i sampled by self-returning paths of length N as illustrated in Fig. 1. The concept of moments is well established in statistics to

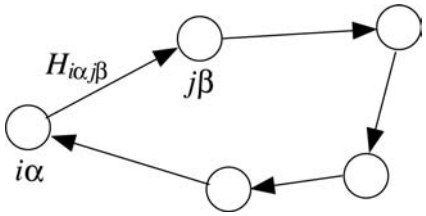

Fig. 1. A self-returning path of length 5 that contributes to the 5-th moment of orbital $i\alpha$.

describe the properties of a distribution and is used in BOP theory to approximate the local DOS, as will be described in the next sections. Higher moments correspond to increasing the length of the hopping paths and hence the sampling of the atomic environment further away from atom i. As will be discussed later on, an analysis of the structural energy differences in terms of moments enables one to relate directly differences in crystal structure to differences in electronic structure.

3.2. Transformation of the Hamilton operator to tridiagonal form

An alternative but mathematically equivalent way of relating the electronic structure to the crystal structure with the help of the moments theorem is the recursion method [10]. Here, the Hamilton operator is transformed to tridiagonal form by recursively generating an appropriate basis, starting from atomic orbital $|u_0\rangle = |i\alpha\rangle$,

$$b_{n+1}|u_{n+1}\rangle = \left(\hat{H} - a_n\right)|u_n\rangle - b_n|u_{n-1}\rangle \tag{12}$$

In this new basis, the Hamilton operator takes the tridiagonal form

$$\langle u_n|\hat{H}|u_m\rangle = \begin{pmatrix} a_0 & b_1 & & & & & \\ b_1 & a_1 & b_2 & & & 0 & \\ & b_2 & a_2 & b_3 & & & \\ & & b_3 & a_3 & b_4 & & \\ & & & b_4 & a_4 & \ddots & \\ & 0 & & & \ddots & \ddots & \ddots \\ & & & & & \ddots & \ddots \end{pmatrix}$$

with the matrix elements

$$a_n = \langle u_n|\hat{H}|u_n\rangle \quad \text{and} \tag{13}$$

$$b_n = \langle u_n|\hat{H}|u_{n-1}\rangle = \langle u_{n-1}|\hat{H}|u_n\rangle \tag{14}$$

The procedure of transforming the Hamilton operator to tridiagonal form is known as the Lanczos algorithm [11]. The tridiagonal form of the Hamilton matrix can be pictorially understood as a semi-infinite one-dimensional nearest-neighbour chain, see Fig. 2. As discussed in the next sections, the numerical BOPs establish an approach for calculating the local electronic density of states and scale linearly with the number of atoms involved. The N-th moment is given as the sum of possible self-returning paths of length N which start on $|u_0\rangle$,

$$\mu_{i\alpha}^{(N)} = \langle u_0|\hat{H}^N|u_0\rangle \tag{15}$$

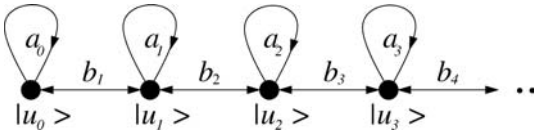

Fig. 2. A graphical illustration of the tridiagonal Hamilton operator that is generated by recursion.

For example, for $N = 2$, $N = 3$, and $N = 4$ one obtains

$$\mu_{i\alpha}^{(2)} = a_0^2 + b_1^2 \tag{16}$$

$$\mu_{i\alpha}^{(3)} = a_0^3 + 2a_0b_1^2 + a_1b_1^2 \tag{17}$$

$$\mu_{i\alpha}^{(4)} = a_0^4 + 3a_0b_1^2 + 2a_0a_1b_1^2 + a_1^2b_1^2 + b_1^2b_2^2 \tag{18}$$

3.3. Construction of the density of states from the moments

For the calculation of the bond energy, the density of states is constructed from the moments. This is achieved by making use of the Green's function $\hat{G}$,

$$\hat{G} = \left(E\hat{1} - \hat{H}\right)^{-1} \tag{19}$$

The density of states may be related to the diagonal matrix elements of the Green's function

$$n_{i\alpha}(E) = -\frac{1}{\pi}\,\mathrm{Im}\,G_{i\alpha i\alpha}(E) \tag{20}$$

in terms of moments by choosing $|u_0\rangle = |i\alpha\rangle$ in the Lanczos recursion. $G_{i\alpha i\alpha}$ may then be written as a continued fraction expansion,

$$G_{i\alpha i\alpha} = G_{00} = \cfrac{1}{E - a_0 - \cfrac{b_1^2}{E - a_1 - \cfrac{b_2^2}{E - a_2 - \cfrac{b_3^2}{\ddots}}}} \tag{21}$$

Hence, the density of states is obtained from the coefficients of the tridiagonal Hamilton operator. A detailed review of the connection between bond-order potentials, Green's functions and the recursion method is given, e. g., in Refs. [12–14].

3.4. Truncation of the continued fraction

The exact solution of the tight-binding problem can in principle be obtained by taking the continued fraction (Eq. (21)) to an infinite number of levels n. An approximate solution can be obtained by *terminating* the continued fraction after a certain number of levels. This leads to a *local* expansion of the electronic structure. The simplest way of terminating the recursion after n levels (i. e. $2n + 1$ moments) is to use a constant terminator

$$a_m = a_\infty,\ b_m = b_\infty \quad \text{for } m > n \tag{22}$$

The error with respect to the exact solution of the TB model will become smaller with more recursion levels n taken into

account. Therefore, the number of recursion levels provides a systematic way for converging the resulting DOS to the DOS that one obtains from an exact solution of the TB model.

3.5. Evaluation of the bond energy

The bond energy may be obtained by integrating an approximate representation of the DOS either numerically or analytically. Therefore, the different approaches of calculating the bond energy are grouped in numerical and analytic bond-order potentials.

3.5.1. Numerical bond-order potentials

Inserting the continued fraction (Eq. (21)) in the Green's function representation of the density of states (Eq. (20)) gives an expression for the bond energy (Eq. (9)). In general, the integral in Eq. (9) has to be carried out numerically, therefore, this approach is referred to as numerical BOP. The calculation of forces is carried out in the intersite representation that is equivalent to the onsite representation of the bond energy [15]. The numerical BOPs are implemented in the program package OXON [12]. A detailed review of the numerical bond-order potentials is available in Ref. [3].

3.5.2. Analytic bond-order potentials

The analytic bond-order potentials express the bond energy explicitly in terms of the atomic positions, i. e. without the need for a numerical integration of the DOS. Two flavours of analytic bond-order potentials were derived. One way is to terminate the recursion expansion Eq. (21) for the density matrix at two levels of recursion corresponding to four moments. Then an analytic integration of the continued fraction expansion is possible. In order to achieve a good convergence of the continued fraction expansion at only two recursion levels, the recursion is started from $|u_0\rangle$ taken as a linear combination of two orbitals, i. e. a dimer orbital [16, 17]. In this way, a good convergence for covalent bonds in sp-valent materials is obtained [2]. This flavour of analytic bond-order potentials is called bond-based. If the expansion is terminated at the second moment level, a format of the analytic bond-order potential is obtained that is very close to the empirical Tersoff potential [18, 19]. The analytic BOP for sp-valent systems therefore are a systematic extension of Tersoff-type potentials.

For unsaturated bonds in close-packed transition metals a different expansion was recently devised that is able to take into account higher moment contributions than the fourth moment [20]. This allows one, e. g., to include six moments that are required to differentiate between the fcc and the hcp structure. The expansion is based on the representation of the DOS in terms of Chebyshev polynomials which may be integrated analytically for analytic expression of the bond energy and the bond order. As the expansion is taken with respect to an atomic orbital that is included in the electronic structure generated by the surrounding atoms, these bond-order potentials are called analytic atom-based BOPs.

The lowest-order approximation of the atom-based analytic bond-order potential for two moments is similar to the Finnis–Sinclair potential [21]. Therefore, the analytic BOP expansion may be viewed as a systematic extension of the Finnis–Sinclair potential to include higher moments. The analytic atom-based BOP formalism is implemented in the program package BOPfox.

3.6. Structural energy difference theorem

The calculation of the binding energy within the tight-binding bond model (Eq. (5)) requires knowledge of the bond energy, the promotion energy and the repulsive energy. Under certain assumptions, however, the differences in the binding energy of different crystal structures can be approximately evaluated *without* knowledge of the repulsive contribution to the binding energy: The structural energy difference theorem [22] states that the energy difference between two structures to first order is given by

$$\Delta U^{(1)} = [\Delta U_{\mathrm{bond}}]_{\Delta U_{\mathrm{rep}}=0} \tag{23}$$

Often the repulsive energy may be approximated as

$$U_{\mathrm{rep}} \propto z\beta^n(R) \tag{24}$$

where z is the number of nearest-neighbour atoms and $\beta(R)$ is the bond integral at nearest-neighbour distance R. With

$$\mu_2 \propto z\beta^2(R) \tag{25}$$

the repulsive energy of two structures is identical if

$$z_1\beta^n(R_1) = z_2\beta^n(R_2) \tag{26}$$

or

$$\mu_2^{(2)} = \left(\frac{z_1}{z_2}\right)^{2n-1} \mu_1^{(2)} \tag{27}$$

Hence, employing a canonical TB model, assuming an appropriate repulsive part and adjusting the second moments allows one to compare the relative stability of different crystal structures as a function of bandfilling. The advantage of such a study of structural trends for a series of chemical elements is that no explicit parametrisation of the repulsive term is needed. In the next section we will present studies of structural trends that are based on the structural energy difference theorem.

4. Application of BOPs to the prediction of structural trends

4.1. sp-valent elements

The analytic bond-order potential for sp-valent systems depends explicitly on the bandfilling and correctly reproduces the structural trend from close-packed to diamond, to 3-fold, 2-fold and 1-fold coordinated structures [23]. The latter was demonstrated by making use of the structural energy difference theorem. A comparison of the structural trends obtained with tight-binding and the analytic bond-order potential (Fig. 3) shows that the bond-order potential predicts the valence-driven structural trends in good agreement with the reference TB calculations.

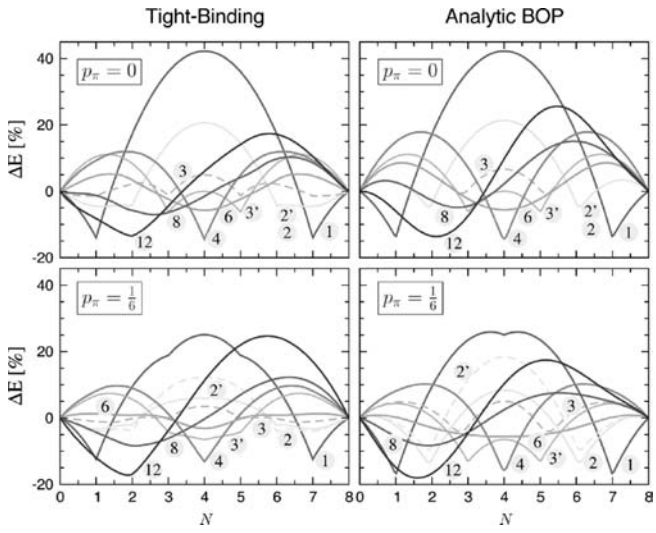

Fig. 3. The structural trends of sp-valent systems with respect to bandfilling as predicted by TB (left) and analytic BOP (right). (Reprinted figure from Ref. [23]. Copyright (2005) by the American Physical Society.)

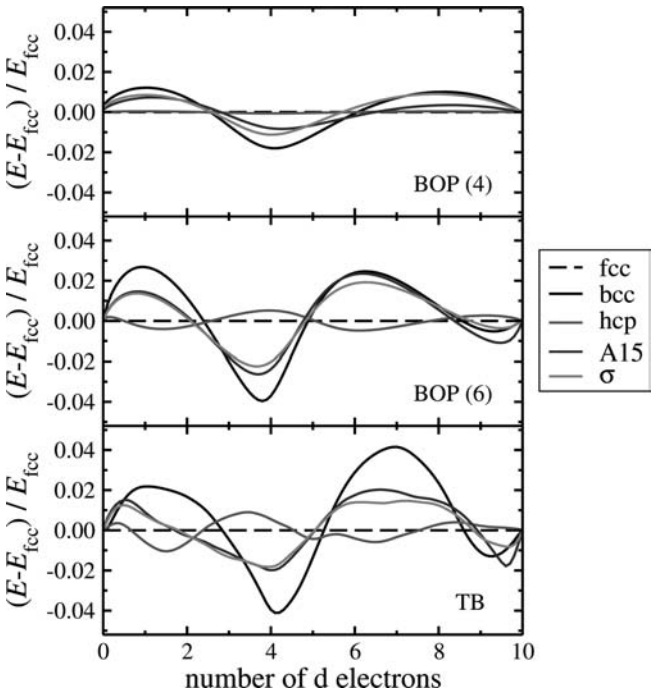

Fig. 4. Convergence of structural energy differences obtained with analytic BOP in comparison to TB for simple and complex phases.

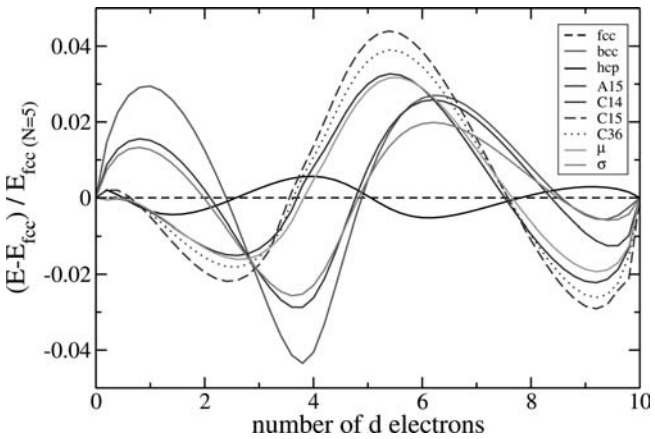

Fig. 5. Predicted structural stability of topologically close-packed phases as a function of the valence obtained with analytic bond-order potentials using six moments. (Reprinted figure from Ref. [26]. Copyright (2008) by The Minerals, Metals & Materials Society.)

4.2. d-valent metals

The analytic bond-order potentials developed for d-valent systems [20] were recently applied to study the structural stability of the structurally complex topologically close-packed (tcp) phases [24]. The precipitation of these phases in Ni-based superalloys for high-temperature applications (see e. g. Ref. [25]) is detrimental to the mechanical properties of the alloys. Structure maps based on experimentally observed phases suggest that the bandfilling is important for the structural stability of the tcp phases [26]. The bandfilling dependence is also observed in density-functional theory calculations of transition metal elements [27] and binary compounds [28].

The bandfilling dependence of the structural stability was studied in the framework of BOPs based on a canonical TB model. Systematic convergence tests of energy differences with respect to number of moments showed that six moments are sufficient to resolve the energy differences between the simple bcc, fcc, hcp lattices [20], as well as the tcp phases A15 and σ [26, 29] as shown in Fig. 4. A more detailed study [26] including further tcp phases reveals distinct groups of tcp-phases that exhibit a similar dependence on bandfilling: A15/σ on one hand and μ/C14/C15/C36 on the other hand (Fig. 5).

5. Application of BOPs for specific materials

In addition to the trends studied in the previous section, bond-order potentials were applied in numerous quantitative studies of materials. Comprehensive reviews on the application of BOPs for metals [3], hydrocarbons [4], and semiconductors [2] have been published recently. In the following, we will summarise briefly a few examples of the application of BOPs.

5.1. hcp transition metal: Ti

One of the first bond-order potentials for transition metals was developed by Girshick [30] for titanium, motivated by the fact that central-force potentials for Ti (see e. g. Refs. [31, 32]) cannot reproduce the experimentally observed dislocation core configuration and preferred slip system [33]. The authors employed a sequential procedure for fitting the tight-binding parameters: First, the bonding part was determined by

(i) adjusting the prefactor of the underlying canonical tight-binding model to reproduce the band width of hcp-Ti,
(ii) determining the number of moments that reproduces the relative stability of hcp, fcc, and bcc, and
(iii) fitting the decay of the bond integrals to the Cauchy pressures.

Second, the repulsive part was fitted to reproduce the hcp-Ti lattice constant, the binding energy and the elastic con-

stants that were not yet determined by the previously fitted Cauchy pressures. This numerical BOP performed qualitatively better in the description of screw dislocations than Finnis-Sinclair-type potentials [33]. In particular, the non-central character of the Ti d-electrons gives rise to a high energy of the intrinsic stacking fault on the basal plane which makes the prism plane the preferred slip plane. As this behaviour is driven by the angular bonding character, it cannot be described with central-force models of the atomic interaction.

5.2. bcc transition metals: Mo and W

More recently, bond-order potentials were developed for the bcc transition metals molybdenum [34] and tungsten [35]. The fitting employed ab-initio reference data for determining the bond integrals. An environment-dependent repulsive term was used to capture the Cauchy pressure of the ground state structure bcc of Mo and W. The repulsive term was fitted to the lattice constant, the binding energy and the elastic constants that were not yet determined by the previously fitted Cauchy pressure. The transferability of the numerical BOPs is demonstrated by showing that they reproduce the relative stability of bcc-A15-fcc-hcp-sc as a function of bandfilling, although they were fitted explicitly only to the ground state structure bcc of Mo and W. Both potentials capture γ surfaces, as well as trigonal, tetragonal and hexagonal transformation paths in good agreement with density-functional theory calculations as shown in Fig. 6 for the case of Mo. Application of the Mo-BOP to the $1/2\langle 111\rangle$ screw dislocation shows very good agreement with ab-initio calculations of both, core structure and dislocation motion [34]. The W-BOP also shows the correct relative stability of different low-index surfaces [35].

5.3. fcc transition metal: Ir

The bond-order potential parametrisation for iridium [36] required to account properly for the hybridisation between the nearly free-electron sp-band and the unfilled d-band. Tests with an spd tight-binding model showed that the hybridisation may be modelled accurately by an additional pairwise central-force term. Parametrisation and testing of the numerical BOP for iridium was carried out as outlined above for Mo and W. In particular, the BOP for iridium reproduces the experimentally observed, anomalous phonon spectrum as shown in Fig. 7. The anomalies in the $[\zeta\zeta 0]$ branch are due to the strong angular bonding character and are correctly described by the numerical BOP. Simulations with this numerical BOP revealed that the strong directional bonding gives rise to high rates of cross slip due to athermal transformation between two screw-dislocation core structures [37]. This results in an exceptionally high rate of dislocation multiplication which explained the unusual brittle fracture that Ir shows after plastic deformation.

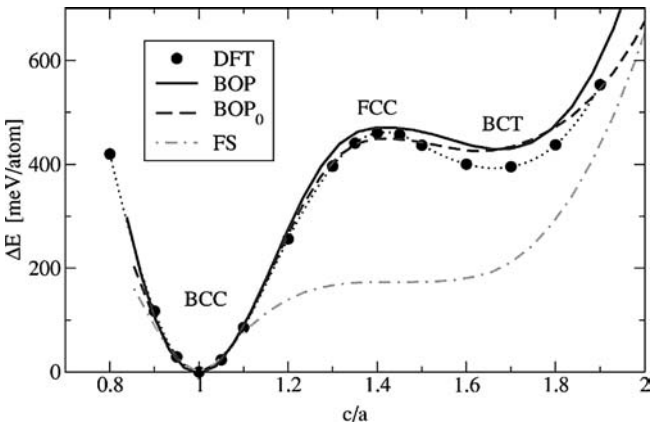

Fig. 6. Energy along the tetragonal transformation path in tungsten as obtained with numerical BOP, unscreened numerical BOP (BOP_0), ab-initio calculations (DFT) and a Finnis-Sinclair potential (FS) [35]. (Reprinted figure with permission from M. Mrovec, R. Gröger, A. G. Bailey, D. Nguyen-Manh, C. Elsässer, and V. Vitek, Phys. Rev. B 75, 104119, 2007. Copyright (2007) by the American Physical Society.)

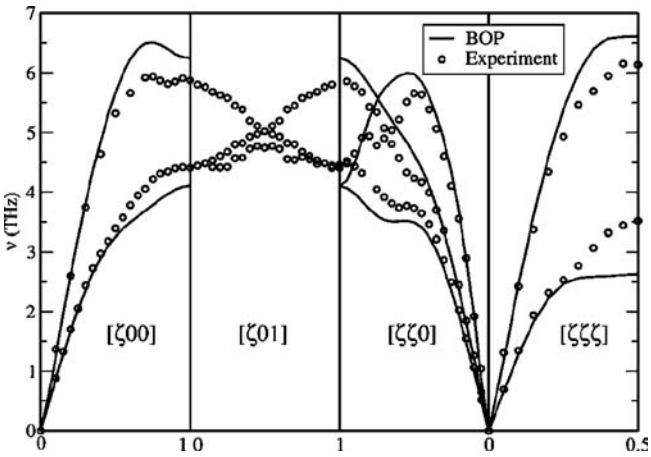

Fig. 7. Phonon spectrum of Ir as obtained from numerical BOP and experiment. (Reprinted figure from Ref. [36]. Copyright (2006) by the American Physical Society.)

5.4. Intermetallics: Ti–Al

The bond-order potential for the Ti–Al intermetallic [38] is based on a tight-binding model for pd-bonded compounds [39]. The decay of the bond integrals is approximated by a power-law with parameters obtained from LMTO calculations. Extensive tests demonstrate the transferability of the BOP to different crystal structures of TiAl (including the hexagonal $D0_{19}$ structure) and to Ti-rich stoichiometries that were not included in the fitting procedure. Furthermore, the predicted formation energies of several stacking-fault-like defects (APB, CSF and SISF) are in very good agreement with ab-initio calculations.

5.5. Intermetallics: Mo–Si

The development of the bond-order potential for Mo–Si [40] was motivated by the need for an accurate description of the complex dislocation core structure that causes anomalous deformation under shear strain. Mo is modelled with a d valence, Si with p electrons, similar to the case of Ti–Al. The bond-order potential shows similar transferability to other crystal structures and other stoichiometries as the one for Ti–Al. Therefore, it provides a reliable description of extended defects and is expected to capture the impact of vibrational entropy on the relative structural stability of Mo–Si phases at elevated temperatures [41].

5.6. Hydrocarbons

The first application of analytic bond-order potentials was carried out for the C–H system [16, 42]. In contrast to earlier empirical potentials for carbon, this analytic BOP explains structural trends driven by the σ bond and correctly describes the breaking of the π bond on radical formation or under torsion [16]. The parametrisation is built on a tight-binding model with implicit screening [43]. By making use of the reduced TB approximation [44]

$$\mathrm{sp}\sigma \cdot \mathrm{ps}\sigma = \mathrm{ss}\sigma \cdot \mathrm{pp}\sigma, \tag{28}$$

it is assured that only a single σ bond may be formed, such that by taking into account the two π bond orders, the carbon chemistry with triple, double, and single bonds may be described appropriately [42]. Molecular-dynamic simulations with the analytic BOP [4] showed that an appropriate treatment of the carbon s-p level splitting is crucial for capturing the variation of bond-strength with bond-length. The BOP predicts the radial distribution function of liquid C in very good agreement with tight-binding and ab-initio (Car–Parinello molecular dynamics) results (Fig. 8). Further MD simulations of the growth of amorphous C–H films showed that the analytic BOP captures the experimentally known dependence of the amorphous structure on the energy of the deposited molecules.

5.7. Compound semiconductor: Ga–As

Obtaining a transferable description for Ga–As that is suitable for modelling the growth of thin films is challenging particularly due to the different surface reconstructions that exist for GaAs as a function of As vapour pressure. The analytic bond-order potential for Ga–As [45] introduced an additional term to the energy in order to mimic the electron counting rule that may be used to describe the relative stability of different surface reconstructions. The parameters of the BOP were fitted to the variation of bond energy with bond length in a first step and to properties determined by angular terms in the second step [46]. The potential predicts defect energies, surface energies and the melting temperature in good agreement with ab-initio and experimental data. Application of the analytic BOP in molecular-dynamic (MD) simulations of GaAs growth in molecular-beam epitaxy (see Fig. 9) revealed a strong relationship between deposition conditions and film quality. In particular, the experimentally known combination of temperature and Ga/As flux ratio that optimises the quality of the film crystallinity was predicted from MD simulations.

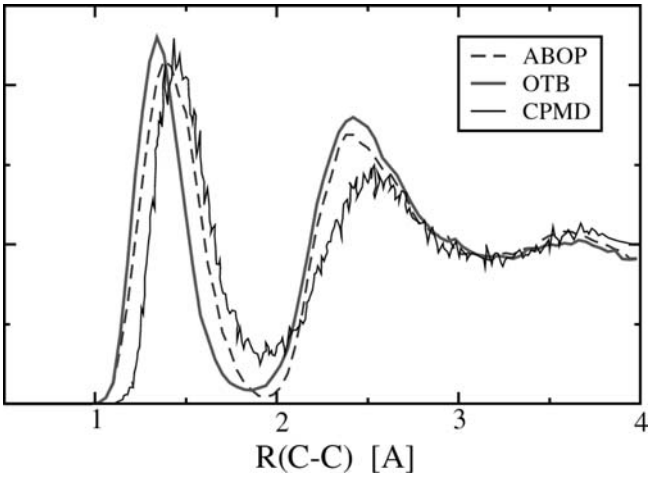

Fig. 8. Comparison of radial distribution function of liquid carbon as obtained with analytic BOP, orthogonal TB, and Car–Parinello ab-initio molecular-dynamic simulations (CPMD). (Reprinted figure from Prog. Mat. Sci. 52, M. Mrovec, M. Moseler, C. Elsässer, and P. Gumbsch, *Atomistic modeling of hydrocarbon systems using analytic bond-order potentials*, 230–254, Copyright (2007), with permission from Elsevier.)

5.8. Elemental semiconductor: Si

The development of the bond-order potential for Si [47] was motivated by the need for a more detailed atomistic understanding of the growth mechanisms in molecular-beam epitaxy. This required a robust and transferable description of the bond formation in Si from the atom to the solid. The strategy for fitting the BOP parameters differed from the case of GaAs in that all parameters were optimised simultaneously to experimental and ab-initio reference data. The transferability of the potential was then validated for a broad range of clusters and bulk structures (Fig. 10), and by demonstrating that the BOP gives a good prediction of the melting temperature. The most notable achievements are the correct prediction of the transition to the β-Sn phase at high pressures and the negative Cauchy pressure which is attributed to the promotion energy. The authors could also demonstrate that the BOP correctly reproduces the surface energies of several reconstructions of the (001) surface with

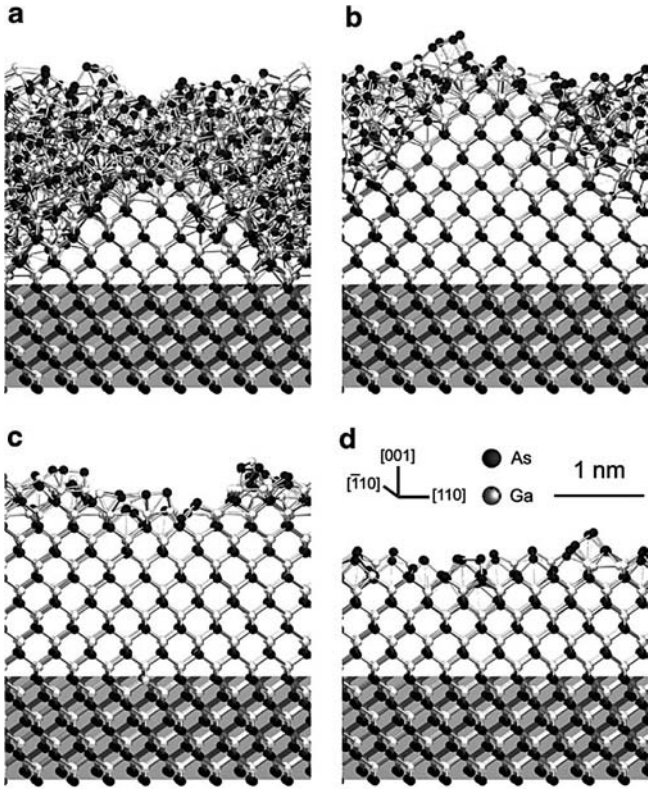

Fig. 9. Snapshots of molecular-dynamic simulations of the growth of GaAs films with analytic BOP. (Reprinted figure from Ref. [2]. Copyright (2007) by Elsevier.)

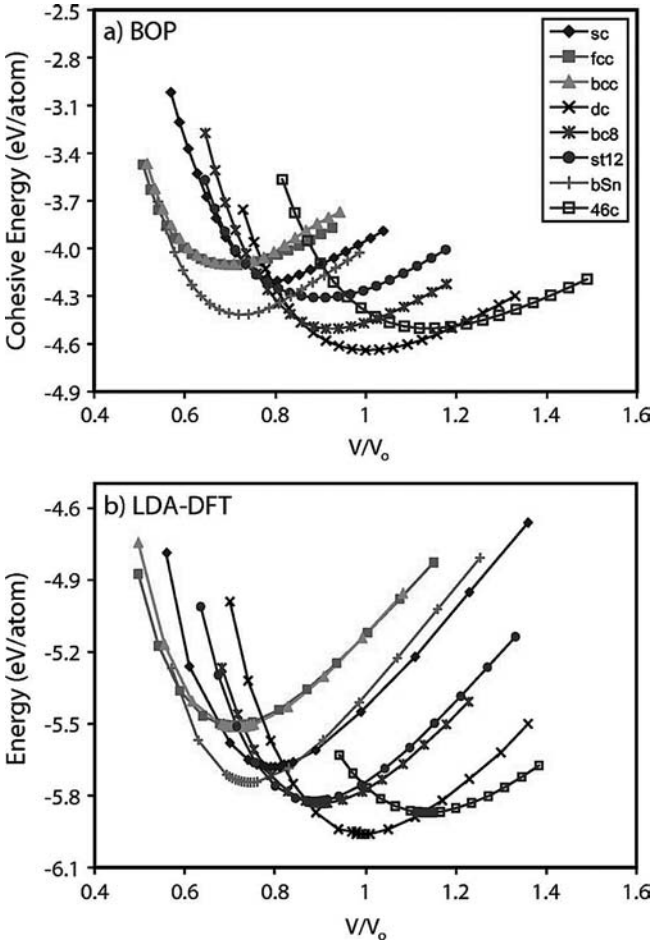

Fig. 10. Comparison of the stability of Si in different crystal structures using (a) BOPs and (b) density-functional theory in the local-density approximation. (Reprinted figure from Ref. [47]. Copyright (2007) by the American Physical Society.)

good agreement to ab-initio calculations. Molecular-dynamic simulations with this analytic bond-order potential confirmed the experimental finding of improved film crystallinity at elevated substrate temperatures during film growth [2].

6. Conclusions

We reviewed the derivation and application of bond-order potentials for sp-valent semiconductors, hydrocarbons and for d-valent transition metals. The bond-order potentials are derived from density-functional theory by coarse-graining the electronic structure at two levels of approximation. In a first step, DFT is coarse-grained into the tight-binding bond model. In a second step, the bond-order potential expansion provides a local interatomic potential based on the relation of the electronic structure to the crystal structure through the moments theorem. As the bond-order potentials are derived from the electronic structure, they depend explicitly on the number of valence electrons. By varying the bandfilling, systematic studies of the trends of crystal structure stability may be carried out. The transferability of the BOPs to different bonding environments has been proven in complex bonding situations for both, elemental and compound systems of metals, hydrocarbons and semiconductors. Current work includes the extension to magnetism and charge transfer.

T.H. and R.D. acknowledge financial support through ThyssenKrupp AG, Bayer MaterialScience AG, Salzgitter Mannesmann Forschung GmbH, Robert Bosch GmbH, and the state of North-Rhine Westphalia as well as the European Comission in the framework of the European Regional Development Fund (ERDF).

References

[1] A.P. Sutton, M.W. Finnis, D.G. Pettifor, Y. Ohta: J. Phys. C 21 (1988) 35.
[2] R. Drautz, X.W. Zhou, D.A. Murdick, B. Gillespie, H.N.G. Wadley, D.G. Pettifor: Prog. Mat. Sci. 52 (2007) 196. DOI:10.1016/j.pmatsci.2006.10.013
[3] M. Aoki, D. Nguyen-Manh, D.G. Pettifor, V. Vitek: Prog. Mat. Sci. 52 (2007) 154. DOI:10.1016/j.pmatsci.2006.10.004
[4] M. Mrovec, M. Moseler, C. Elsässer, P. Gumbsch: Prog. Mat. Sci. 52 (2007) 230. DOI:10.1016/j.pmatsci.2006.10.012
[5] M.W. Finnis: Prog. Mat. Sci. 52 (2007) 133. DOI:10.1016/j.pmatsci.2006.10.003
[6] T. Hammerschmidt, R. Drautz, in: NIC Series 42 – Multiscale Simulation Methods in Molecular Science, edited by J. Grotendorst, N. Attig, S. Blügel, D. Marx (Jülich Supercomputing Centre, 2009), 229.
[7] D. Nguyen-Manh, D.G. Pettifor, V. Vitek: Phys. Rev. Lett. 85 (2000) 4136. PMid:11056643; DOI:10.1103/PhysRevLett.85.4136
[8] D.G. Pettifor, Bonding and Structure of Molecules and Solids (Oxford Science Publications, 1995).
[9] F. Cryot-Lackmann: Adv. Phys. 16 (1967) 393. DOI:10.1080/00018736700101495
[10] R. Haydock: Comp. Phys. Comm. 20 (1980) 11. DOI:10.1016/0010-4655(80)90101-0
[11] C. Lanczos: J. Res. Natl. Bur. Stand. 45 (1950) 225.
[12] A. Horsfield, A.M. Bratkovsky, M. Fearn, D.G. Pettifor, M. Aoki: Phys. Rev. B 53 (1996) 12694. DOI:10.1103/PhysRevB.53.12694
[13] D.G. Pettifor: Phys. Rev. B 63 (1989) 2480. PMid:10040899; DOI:10.1103/PhysRevLett.63.2480
[14] M.W. Finnis: Interatomic forces in condensed matter (Oxford University Press, Oxford, 2007).
[15] M. Aoki: Phys. Rev. Lett. 71 (1993) 3842. PMid:10055087; DOI:10.1103/PhysRevLett.71.3842
[16] D.G. Pettifor, I.I. Oleinik: Phys. Rev. B 59 (1999) 8487. DOI:10.1103/PhysRevB.59.8487
[17] D.G. Pettifor, I.I. Oleinik: Phys. Rev. Lett. 84 (2000) 4124. PMid:10990626; DOI:10.1103/PhysRevLett.84.4124
[18] P. Alinaghian, P. Gumbsch, A.J. Skinner, D.G. Pettifor: J. Phys. Cond. Mat. 5 (1993) 5795. DOI:10.1088/0953-8984/5/32/010
[19] J. Tersoff: Phys. Rev. Lett. 56 (1986) 632. PMid: 10033244; DOI:10.1103/PhysRevLett.56.632
[20] R. Drautz, D.G. Pettifor: Phys. Rev. B 74 (2006) 174117. DOI:10.1103/PhysRevB.74.174117
[21] M.W. Finnis, J.E. Sinclair: Phil. Mag. A 50 (1984) 45. DOI:10.1080/01418618408244210
[22] D.G. Pettifor: J. Phys. C 19 (1986) 285.
[23] R. Drautz, D.A. Murdick, D. Nguyen-Manh, X.W. Zhou, H.N.G. Wadley, D.G. Pettifor: Phys. Rev. B 72 (2005) 144105. DOI:10.1103/PhysRevB.72.144105
[24] A.K. Sinha: Prog. Mat. Sci. 15 (1973) 79.
[25] C.M.F. Rae, R.C. Reed: Acta. Mat. 49 (2001) 4113. DOI:10.1016/S1359-6454(01)00265-8
[26] T. Hammerschmidt, B. Seiser, R. Drautz, D.G. Pettifor, in: Superalloys 2008, edited by R.C. Reed, K. Green, P. Caron, T. Gabb, M. Fahrmann, E. Huron, S.Woodward: The Metals, Minerals and Materials Society (2008), 847.
[27] C. Berne, A. Pasturel, M. Sluiter, B. Vinet: Phys. Rev. Lett. 83 (1999) 1621. DOI:10.1103/PhysRevLett.83.1621
[28] T. Hammerschmidt, B. Seiser, R. Drautz, D.G. Pettifor: in preparation.
[29] P.E.A. Turchi: Mat. Res. Soc. Symp. Proc. 206 (1991) 265.
[30] A. Girshick, A.M. Bratkovsky, D.G. Pettifor, V. Vitek: Phil. Mag. A 77 (1998) 981. DOI:10.1080/01418619808221223
[31] G. Ackland: Phil. Mag. A 66 (1992) 917. DOI:10.1080/01418619208247999

[32] T. Hammerschmidt, A. Kersch, P. Vogl: Phys. Rev. B 71 (2005) 205409. DOI:10.1103/PhysRevB.71.205409
[33] A. Girshick, D.G. Pettifor, V. Vitek: Phil. Mag. A 77 (1998) 999. DOI:10.1080/01418619808221224
[34] M. Mrovec, D. Nguyen-Manh, D.G. Pettifor, V. Vitek: Phys. Rev. B 69 (2004) 094115. DOI:10.1103/PhysRevB.69.094115
[35] M. Mrovec, R. Gröger, A.G. Bailey, D. Nguyen-Manh, C. Elsässer, V. Vitek: Phys. Rev. B 75 (2007) 104119. DOI:10.1103/PhysRevB.75.104119
[36] M.J. Cawkwell, D. Nguyen-Manh, D.G. Pettifor, V. Vitek: Phys. Rev. B 73 (2006) 064104. DOI:10.1103/PhysRevB.73.064104
[37] M.J. Cawkwell, D. Nguyen-Manh, C. Woodward, D.G. Pettifor, V. Vitek: Science 309 (2005) 1059. PMid: 16099981; DOI:10.1126/science.1114704
[38] S. Znam, D. Nguyen-Manh, D.G. Pettifor, V. Vitek: Phil. Mag. 83 (2003) 415. DOI:10.1080/0141861021000054601
[39] D.G. Pettifor, R. Podloucky: Phys., Rev. Lett. 53 (1994) 1080. DOI:10.1103/PhysRevLett.53.1080
[40] M.J. Cawkwell, M. Mrovec, D. Nguyen-Manh, D.G. Pettifor, V. Vitek: Mater. Res. Soc. Symp. Proc. 842 (2005) S.2.8.1.
[41] Y. Chen, T. Hammerschmidt, D.G. Pettifor, J.-X. Shang, Y. Zhang: Acta Mat. 57 (2009) 2657. DOI:10.1016/j.actamat.2009.02.014
[42] I.I. Oleinik, D.G. Pettifor: Phys. Rev. B 59 (1999) 8500. DOI:10.1103/PhysRevB.59.8500
[43] L. Goodwin, A.J. Skinner, D.G. Pettifor: Europhys. Lett. 9 (1989) 701. DOI:10.1209/0295-5075/9/7/015
[44] D.G. Pettifor, M.W. Finnis, D. Nguyen-Manh, D.A. Murdick, X.W. Zhou, H.N.G. Wadley: Mater. Sci. Eng. A 365 (2004) 2. DOI:10.1016/j.msea.2003.09.001
[45] D.A. Murdick, X.W. Zhou, H.N.G.Wadley, D. Nguyen-Manh, R. Drautz, D.G. Pettifor: Phys. Rev. B 73 (2006) 045206. DOI:10.1103/PhysRevB.73.045206
[46] K. Albe, K. Nordlund, J. Nord, A. Kuronen: Phys. Rev. B 66 (2002) 035205. DOI:10.1103/PhysRevB.66.035205
[47] B. Gillespie, X.W. Zhou, D.A. Murdick, H.N.G. Wadley, R. Drautz, D.G. Pettifor: Phys. Rev. B 75 (2007) 155207. DOI:10.1103/PhysRevB.75.155207

(Received August 23, 2009; accepted September 15, 2009)

Bibliography

DOI 10.3139/146.110207
Int. J. Mat. Res. (formerly Z. Metallkd.)
100 (2009) 11; page 1479 – 1487

ISSN 1862-5282

Correspondence address

Dr. Thomas Hammerschmidt
Interdisciplinary Centre for Advances Materials Simulation (ICAMS)
Ruhr-University Bochum
44780 Bochum, Germany
Tel.: +49 234 32 29375
Fax: +49 234 32 14977
E-mail: thomas.hammerschmidt@rub.de

You will find the article and additional material by entering the document number **MK110207** on our website at *www.ijmr.de*